Real-Time Estimation of Food Defrosting by Software Sensors

E. Akkari, S. Chevallier, and L. Boillereaux
GEPEA, UMR CNRS 6144, ENITIAA, rue de la Géraudière, BP 82225, F- 44322 Nantes cedex 3, France

DOI 10.1002/aic.10759
Published online January 13, 2006 in Wiley InterScience (www.interscience.wiley.com).

*Software sensors (or observers) are especially useful when the state vector of a system cannot be measured. Widely employed for bioprocesses, they estimate the state variables from available measurements, which are functions of one or several state variables, provided that the observability property is checked. In food defrosting, an important challenge is to know the spread of the melting front inside the product, without any invasive measurement. The solution proposed in this paper is based on the design of software sensors able to estimate, from a superficial temperature measurement, the temperature distribution in the product, in real time, and consequently making it possible to determine the melting zone. The proposed solutions are, first, an extended Kalman Filter and, second, switched reduced Luenberger observers. The results are illustrated during the experimental thawing of a block of tylose in forced convection.**AIChE J,* 52: 1473–1480, 2006
Keywords: Luenberger observer, Extended Kalman Filter, heat transfer, phase change, thawing.

Introduction

Freezing[1] and defrosting are key operations for the food industry, in that they represent the most employed technique for food preservation in industrial countries. To be able to measure the position of the melting or crystallization front in real time can prove very beneficial for the process, as it enables one to supervise the progress inside the food, or better still, to control the kinetics of it[1,2]. Indeed, some authors reported that the kinetics of freezing or defrosting has a considerable influence on the final quality of the product, whether it is from the organoleptic point of view or in terms of drip losses[3,4].

To our best knowledge, no relevant technical solution, which is not invasive, is available today to achieve this goal. In this paper, we propose to estimate this front location from the single knowledge of the superficial temperature of the product. An algorithmic treatment associated with this measurement makes it possible to develop a software sensor.

Correspondence concerning this article should be addressed to L. Boillereaux at boil@enitiaa-nantes.fr.

Software sensors, more known under the denomination "observers" in the process control community, were the subject of many works in the past 50 years. They have been applied to a broad variety of model structures. Relevant analytical solutions are proposed for linear systems, as the famous Luenberger observer[5], the Kalman Filter[6], or the Least-Squares approaches[7,8]. As for nonlinear systems, the most employed approach is certainly the Extended Kalman Filter[9]. Analytical solutions are available[10-13], although they ask strong competence in mathematics and require heavy calculations. Finally, some numerical approaches, based on criterion minimization, can be applied to linear or non linear systems[14-16].

However, modeling of heat transfer, with or without phase change, leads to the class of distributed parameters systems, that is, described by partial differential equations. If some authors propose to consider this system in terms of control[17] or observer design[18], the technique most commonly used is to reduce these systems into lumped parameters, via orthogonal collocation, singular perturbations or finite differences, and to apply the observer solutions mentioned previously. No work deals with this problematic with regards to phase change during heat transfer.

In this article, we propose to estimate the melting front location during food thawing, first using the well-known Extended Kalman Filter, and second by proposing a set of switched Luenberger observers. The article is organized as follows:
- Brief recall of observers and observability properties,
- Modelling heat transfer with phase change (including reduction into lumped parameters systems),
- Observability analysis of the system,
- About Extended Kalman Filter and the Switched Luenberger Observers,
- Description of experimental defrosting of tylose in simple geometry under forced convection.

Brief recall about observers

Let us consider the following nonlinear system:

$$\frac{dx}{dt} = f(x(t),\, u(t))$$

$$y = g(x(t)) \tag{1}$$

where $x \in \mathrm{R}^{\mathrm{n}}$ represents the state vector, $u \in \mathrm{R}^{\mathrm{m}}$ the input vector (or manipulated vector) and $y \in \mathrm{R}^{\mathrm{p}}$ the output (or observation) vector. An observer for this system[10] is the following auxiliary dynamical system:

$$\frac{dz}{dt} = f(z(t),\, u(t),\, y(t))$$

$$\hat{x}(t) = g(z(t),\, u(t),\, y(t)) \tag{2}$$

where the input vector is constituted of the input and output vectors of the system, and the output vector $\hat{x}(t)$ is the estimated state vector.

A necessary condition to assign the dynamics of the observer is that the system must be observable, that is, it does not have couples of indistinguishable initial states[10,19].

In the case of linear systems,

$$\frac{dx}{dt} = Ax + Bu$$

$$y = Cx \tag{3}$$

A sufficient and necessary condition of observability is that the observability matrix, defined as in (4), is of full rank.

$$\theta = \begin{bmatrix} C \\ CA \\ \vdots \\ CA^{n-1} \end{bmatrix} \tag{4}$$

For nonlinear systems, this condition is local, and the system (1) is locally observable in x_0 if and only if the rank of

$$\frac{\partial}{\partial x} \left\{ \begin{matrix} g \\ L_f g \\ \vdots \\ L_f^{n-1} g \end{matrix} \right\} \Bigg|_{x_0} \tag{5}$$

is n.

$L_f g$ represents the Lie derivative[20].

Modeling of heat transfer with phase change

Issued from the well-known Fourier's Law, the heat transfer by conduction inside a solid is described by the following equation, where no source term is considered:

$$\rho(T) C_p(T) \frac{\partial T}{\partial t} = \mathrm{div}(\lambda(T)\widetilde{\mathrm{grad}}T) \tag{6}$$

By considering that the thermal conductivity is quite constant except during the melting phase, it can be simplified as follows:

$$\rho(T) C_p(T) \frac{\partial T}{\partial t} = \lambda(T) \cdot \mathrm{div}(\widetilde{\mathrm{grad}}T) \tag{7}$$

Afterwards, only one-dimensional (1-D) heat transfer is considered ("infinite plate"):

$$\rho(T) C_p(T) \frac{\partial T}{\partial t} = \lambda(T) \cdot \frac{\partial^2 T}{\partial z^2} \tag{8}$$

Concerning the boundary conditions, we consider that the heat exchange at the surface in $z = 0$ is convective, and that the surface in $z = L$ is insulated:

$$\begin{cases} \dfrac{\partial T}{\partial z} = 0 & \text{at } z = L \\ h(T_a - T(z)) = -\lambda(T, z) \cdot \dfrac{\partial T}{\partial z} & \text{at } z = 0 \\ T(z, t) = T_0 & \text{at } t = 0, \quad \forall\, z \end{cases} \tag{9}$$

As mentioned in the introduction, works about distributed parameters systems are sparse, especially for nonlinear systems, and the usual approach consists of reducing them into lumped parameters systems. Let us consider a spatial meshing of the food, composed of n homogeneous volumes with δz, their thickness. An energy balance of each volume leads to the following system of equations:

$$\begin{cases} \dfrac{dT_1}{dt} \approx \Psi(T_1)\left(T_2 - T_1\left(1 + \dfrac{h \cdot \delta z}{\lambda(T_1)}\right)\right) + \dfrac{h \cdot \delta z}{\lambda(T_1)} \cdot \Psi(T_1) \cdot T_a \\ \dfrac{dT_i}{dt} \approx \Psi(T_i)(T_{i+1} - 2T_i + T_{i-1}) \quad \forall\, i \in [2;\, n-1] \\ \dfrac{dT_n}{dt} \approx \Psi(T_n)(T_{n-1} - T_n) \end{cases} \tag{10}$$

where

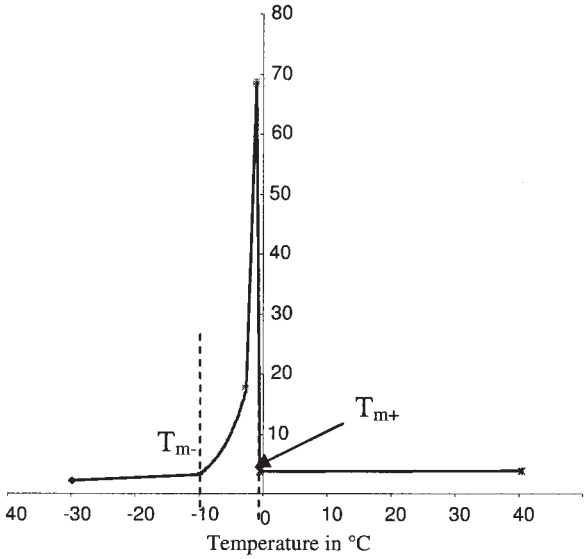

Figure 1. Apparent specific heat of tylose (methylcellulose + water) with temperature

$$\Psi(T) = \frac{\lambda(T)}{\rho(T) \cdot C_p(T) \cdot \delta z^2}$$

For the majority of the foodstuffs, the thermal conductivity and the density remain quite constant with temperature in liquid or solid phases, with a smooth variation during melting phase. On the contrary, the apparent specific heat (taking into account the latent heat), increases considerably during the melting phase. Figure 1 illustrates the result obtained by Differential Scanning Calorimetry for a sample of tylose (water + methylcellulose). T_{m+} corresponds to the peak of apparent specific heat.

Due to the particular form of the apparent specific heat function (Figure 1), let us consider that we can split its evolution in three distinct phases:

(i) The first one corresponds to the solid phase, where the sample is totally frozen:

$$T_i \leq T_{m-} \quad \forall\, i \tag{11}$$

In this phase, thermal properties can be considered constant, even if the specific heat evolves slowly with temperature (Figure 1). The model can be rewritten as a linear state space representation:

$$\frac{dT}{dt} = AT + Bu \tag{12}$$

where A is a three-diagonal matrix and u is the ambient temperature:

$$A = \Psi_f \cdot \begin{bmatrix} -1 - \dfrac{h \cdot \delta z}{\lambda_f} & 2 & 0 & 0 & \cdots & 0 \\ 1 & -2 & 1 & 0 & \cdots & 0 \\ 0 & 1 & -2 & 1 & \ddots & \vdots \\ 0 & 0 & \ddots & \ddots & \ddots & \vdots \\ \vdots & \vdots & \ddots & 1 & -2 & 1 \\ 0 & 0 & \cdots & 0 & 1 & -1 \end{bmatrix};$$

$$B = \begin{bmatrix} \dfrac{h \cdot \delta z}{\lambda_f} \cdot \Psi_f \\ 0 \\ \vdots \\ 0 \end{bmatrix} \tag{13}$$

(ii) The second one corresponds to the melting phase, and the model is Eq. 10 if at least one temperature T_i verifies the following inequalities:

$$T_{m-} < T_i < T_{m+} \tag{14}$$

(iii) At last, if $T_i \geq T_{m+}$, $\forall i$, the following linear state space representation can be used:

$$A = \Psi_d \cdot \begin{bmatrix} -1 - \dfrac{h \cdot \delta z}{\lambda_d} & 2 & 0 & 0 & \cdots & 0 \\ 1 & -2 & 1 & 0 & \cdots & 0 \\ 0 & 1 & -2 & 1 & \ddots & \vdots \\ 0 & 0 & \ddots & \ddots & \ddots & \vdots \\ \vdots & \vdots & \ddots & 1 & -2 & 1 \\ 0 & 0 & \cdots & 0 & 1 & -1 \end{bmatrix};$$

$$B = \begin{bmatrix} \dfrac{h \cdot \delta z}{\lambda_d} \cdot \Psi_d \\ 0 \\ \vdots \\ 0 \end{bmatrix} \tag{15}$$

Observability analysis

Solid and liquid phases

Let us consider a measurement of the surface at $z = 0$. The output vector is $y = g(T_1) = T_1$, the output equation of both linear state space representations is:

$$y = C \cdot T \tag{16}$$

with

$$C = [1 \quad 0 \quad \cdots \quad 0]$$

It can be verified that the observability matrix is triangular, with non null coefficients on the diagonal: the rank condition is always verified and the system is thus observable in solid and liquid phases. Indeed, diag(Obs) = [1 2 ⋯ 2].

Melting phase

Let us consider the particular class of nonlinear and upper-triangular systems:

$$\dot{T} = \begin{bmatrix} f_1(T_1, T_2) \\ f_2(T_1, T_2, T_3) \\ \vdots \\ f_{n-1}(T_1, T_2, \ldots, T_{n-1}, T_n) \\ f_n(T_1, T_2, \ldots, T_n) \end{bmatrix} + \sum_i^m \begin{bmatrix} \tilde{f}_{i,1}(T_1) \\ \tilde{f}_{i,2}(T_1, T_2) \\ \vdots \\ \tilde{f}_{i,n}(T_1, T_2, \ldots, T_n) \end{bmatrix} \cdot u_i \quad (17)$$

For an output vector $y = g(T_1)$, a necessary and sufficient condition for this system to be observable is to be at strict bounds[10]. In other words, it means that $\frac{\partial f_i}{\partial T_{i+1}} \neq 0, \ \forall\, i \in [1; n-1]$.

It can be noted straightforwardly that the system issued from the reduction of the heat equation belongs to the class of upper-triangular systems. Let us consider a measurement of the surface at $z = 0$. The output vector is thus $y = g(T_1) = T_1$

Concerning the strict bonds, it appears that: $\frac{\partial f_i}{\partial T_{i+1}} = \Psi(T_i) \ \forall\, i \in [1; n-1]$

From an analytical point of view, the function $\Psi(T)$ is never equal to zero, and the system is thus observable. However, it can be noticed, due to the form of the apparent specific heat, that:

$$\Psi(T) \xrightarrow{T \to T_{m+}} \varepsilon$$

$$\varepsilon \ll \Psi(T) \quad \forall\, T \neq T_{m+}$$

Consequently, when a volume i is at temperature T_{m+}, $\Psi(T_i)$ is close to 0. The dependency of the measurement T_1 with the temperatures T_{i+1} to T_n is thus considerably reduced.

The state space can be split into an observable subspace $(T_{1, \ldots, T_i})$, and another one, $(T_{i+1, \ldots, T_n})$, which is nonobservable from a numerical point of view.

Observer design

In this section we will consider the previous problem in two different ways. First of all, we propose to develop an Extended Kalman Filter, based on the complete nonlinear model ([10]), while keeping in mind that a part of the state will be slightly observable. Second, we propose to benefit from the linearity of the model in the observable part by developing reduced Luenberger observers. In other words, the state estimation is limited to the observable subsystem. Obviously, due to the melting front progression, we propose to use a set of switched reduced observers.

Extended Kalman Filter

Let us consider the nonlinear model ([10]). It can be rewritten in the following matrix form:

$$\frac{dT}{dt} \approx A(T) \cdot T + B(T) \cdot T_a$$

$$y = C \cdot T \quad (18)$$

where A is a three-diagonal matrix $(n \times n)$ with $A_{i,i} = -2\Psi(T_i)$, $A_{i,i+1} = A_{i,i-1} = \Psi(T_i) \ \forall i \in [2, n]$, and $A_{1,1} = -\Psi(T_1)\left(1 + \frac{h \cdot \delta z}{\lambda(T_1)}\right)$, $A_{1,2} = \Psi(T_1) \cdot \frac{h \cdot \delta z}{\lambda(T_1)}$. All the coefficients of B $(1 \times n)$ are equal to zero except $B_1 = \Psi(T_1) \cdot \frac{h \cdot \delta z}{\lambda(T_1)}$. In the same way, all the coefficients of C $(n \times 1)$ are equal to zero except $C_1 = 1$.

The Extended Kalman Filter uses a linearization of the model for the calculation of the gain of the covariance of the estimated state vector. This observer is given by the following structure[9]:

$$\frac{d\hat{T}}{dt} = A(\hat{T})\hat{T}(t) + B(\hat{T})u(t) + K(t)[y(t) - C\hat{T}(t)]$$

$$\text{with} \quad K(t) = P(t)\Lambda^T(t)R^{-1}(t) \quad (19)$$

$K(t)$ is the gain of observer. $\hat{T}(t)$ represents the estimated state vector. The covariance of the estimation error, denoted $P(t)$, must satisfy the Riccati equation[21]:

$$\dot{P}(t) = \Gamma(\hat{T}(t))P(t) + P(t)\Gamma^T(\hat{T}(t)) + Q(t) - P(t)\Lambda^T(\hat{T}(t))R^{-1}(t)\Lambda(\hat{T}(t))P(t) \quad (20)$$

with

$$\Gamma(\hat{T}(t)) = \left.\frac{\partial[A(T)T(t) + B(T)u(t)]}{\partial T(t)}\right|_{T(t)=\hat{T}(t)}$$

$$\Lambda(\hat{T}(t)) = \left.\frac{\partial[CT(t)]}{\partial T(t)}\right|_{T(t)=\hat{T}(t)} \quad (21)$$

It is obvious that in solid and liquid phases, the thermal parameters being constant, we have:

$$\Gamma(\hat{T}(t)) = A$$

$$\Lambda(\hat{T}(t)) = C \quad (22)$$

$Q(t)$ and $R(t)$ are real, symmetric and definite positive matrices, representing the variance of output and state noises, assumed to be white and centred. They are usually fixed arbitrarily, and so a good practice is necessary for their correct adjustment.

Switched reduced Luenberger observers

As mentioned previously, we propose here to limit the state estimation to the observable subsystem. In this subsystem, the function $\Psi(T)$ is quite constant and we can consider that the

Table 1. Thermal and Physical Properties of Tylose

Temperature (°C)	$T < -10$	$-10 \le T \le -2.6$	$-2.6 < T < -1.1$	$-1.1 < T < 0.5$	$0.5 \le T$
Apparent specific heat (KJ/kg · K)	$0.0529 \cdot T + 3.7841$	$31.785 \cdot \exp(0.2306 \cdot T)$	$33.278 \cdot T + 103.71$	$-110.92 \cdot T - 48.561$	$0.0037 \cdot T + 3.6827$
Thermal conductivity (W/m · K)	$1.43/(1 + \exp(1379.4 \cdot T + 5794.5)) + 0.52$				
Density (kg/m^3)	960	1014	1014	1014	1068

model is linear. The model, reduced to the observable subspace, is:

$$\frac{dT^{obs}}{dt} \approx A^{obs} \cdot T^{obs} + B^{obs} \cdot T_a$$

$$y = C^{obs} \cdot T^{obs} \tag{23}$$

where $T^{obs} \in R^k$, by considering that the volumes 1 to k-1 are in the defrosted area, and that the melting area begins at volume k. We can then consider that the temperature at volume k does not evolve due to the small value of $\Psi(T_k)$:

$$\frac{dT_k^{obs}}{dt} = 0$$

For volumes 1 to k-1, $\Psi(T) = \Psi_d$. The matrix A^{obs}, of dimensions $(k \times k)$, is simplified as follows:

$$A^{obs} = \Psi_d \cdot \begin{bmatrix} -1 - \frac{h\delta z}{\lambda} & \frac{h\delta z}{\lambda} & 0 & \cdots & \cdots & 0 \\ 1 & -2 & 1 & \ddots & & \vdots \\ 0 & 1 & -2 & 1 & \ddots & \vdots \\ \vdots & \ddots & \ddots & \ddots & \ddots & 0 \\ \vdots & & \ddots & 0 & 1 & -2 & 1 \\ 0 & \cdots & 0 & 0 & 0 & 0 \end{bmatrix}$$

and $B_1^{obs} = \Psi_d \cdot \frac{h \cdot \delta z}{\lambda_d}$.

The expression of the Luenberger observer[5] is similar to that obtained with the Extended Kalman Filter ([19]), but with a constant gain K:

$$\frac{d\hat{T}^{obs}}{dt} = A^{obs}\hat{T}^{obs}(t) + B^{obs}u(t) + K^{obs} \cdot [y(t) - C^{obs}\hat{T}^{obs}(t)] \tag{24}$$

The convergence rate of the estimation error, $\tilde{T}^{obs}(t) = \hat{T}^{obs}(t) - T^{obs}(t)$, depends on the eigenvalues of the matrix $A^{obs} - K^{obs}C^{obs}$. Indeed,

$$\frac{d\tilde{T}^{obs}}{dt} = (A^{obs} - K^{obs}C^{obs}) \cdot \tilde{T}^{obs}(t) \tag{25}$$

As for the Kalman Filter, certain skills are necessary to correctly determine the matrix K, that is, the eigenvalues of $A^{obs} - K^{obs}C^{obs}$.

Concerning the nonobservable subsystem, from volume $k+1$ to n, we propose a simulation without correction:

$$\frac{d\hat{T}^{no}}{dt} = A^{no}(\hat{T}^{no}) \cdot \hat{T}^{no}(t) + B^{no}(\hat{T}^{no}) \cdot u(t) \tag{26}$$

where A^{no} is a $(n - k) \times (n - k)$ matrix.
Finally, the complete solution we propose is:

$$\frac{d\hat{T}}{dt} = \begin{bmatrix} A^{obs} & 0 \\ 0 & A^{no}(\hat{T}^{no}) \end{bmatrix} \cdot \hat{T}(t) + \begin{bmatrix} B^{obs} \\ B^{no}(\hat{T}^{no}) \end{bmatrix} \cdot u(t) + \begin{bmatrix} K^{obs} \\ 0 \end{bmatrix} \cdot (y - C\hat{T}) \tag{27}$$

with $\hat{T} = \begin{bmatrix} \hat{T}^{obs} \\ \hat{T}^{no} \end{bmatrix}$.

Switching conditions

At the initial time, the temperatures T_1 to T_k are below T_{m+}. No correction is proposed and the evolutions of the temperatures are computed with ([27]), where $A^{obs} \in R^{0\times0}$, $B^{obs} \in R^0$, $K^{obs} \in R^0$ and $A^{no} \in R^{n\times n}$, $B^{no} \in R^n$.

First commutation: $T_1 > T_{m+}$. As soon as the measurement of the superficial temperature is superior to the finishing melting temperature, the melting area starts at volume 2. Equation ([27]) is used for the estimation, with $A^{obs} \in R^{2\times2}$, $B^{obs} \in R^2$, $K^{obs} \in R^2$ and $A^{no} \in R^{(n-2)\times(n-2)}$, $B^{no} \in R^{n-2}$.

Second commutation: $\hat{T}_2 > T_{m+}$. As soon as the estimation of the temperature at volume 2 is superior to the finishing melting temperature, it can be assumed that the melting front starts now at volume 3, and $A^{obs} \in R^{3\times3}$, $B^{obs} \in R^3$, $K^{obs} \in R^3$ and $A^{no} \in R^{(n-3)\times(n-3)}$, $B^{no} \in R^{n-3}$.

Next commutations: $\hat{T}_i > T_{m+}$. The evolution of the dimensions of the matrices continues until $i = n$.

Experimental validation

The Luenberger observers and the Kalman filter have been developed using Matlab® and Simulink® softwares.

Experimental conditions

The product considered in our experiments is Tylose, which is composed of water (86.6 %), methyl cellulose (13%) and salt (0.4%). We present its thermal and physical properties[22] in Table 1.

The tylose sample is 6 cm thick; its lateral and inferior surfaces are perfectly insulated to warrant a unidirectional heat transfer. The block of tylose is located in a climatic chamber where the convective coefficient h is approximately known (30 W/m^2.K) and where the ambient temperature is controlled and measured ($Ta = 30$°C). The initial temperature of the sample is -35°C.

In order to judge the relevance of the approach, 4 thermo-

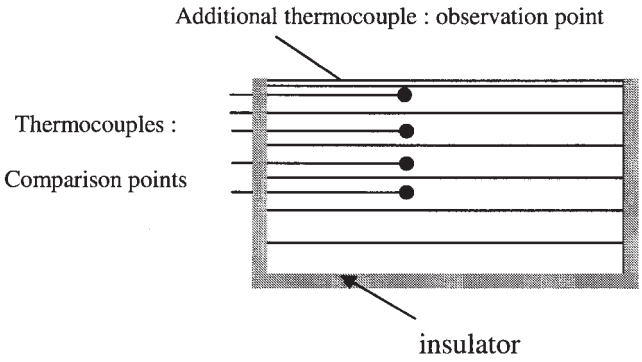

Figure 2. Spatial grid

couples were located inside the block of tylose, to compare estimated and measured temperatures. The first one is 5 mm below the surface. The other thermocouples are 15 mm, 25 mm and 35 mm below the surface and will be used to compare the estimated and measured temperatures. In heat transfer modelling, it is well-known that a refinement of the grid close to the surface is widely beneficial. For this reason, a fifth thermocouple is added as close as possible to the surface ($\approx$1 mm). Thus, the number of finite volumes is equal to 7.

The first volume in this case is 1.5 mm thick, and the second is 3.5 mm thick. The spatial grid used is illustrated in Figure 2.

Experimental results

The initial conditions are voluntarily chosen far from those of sample of tylose, for better appreciating their convergence. Indeed, the initial temperature of the sample during the experiments was -35°C, and the Kalman Filters and switched observers were initialized at -45°C. The temperature corresponding to the thermocouple close to the surface is not represented for a better readability of the figures.

Extended Kalman filter

The matrix Q and R are assumed constant and chosen to obtain a good convergence:

$$Q = 0.1 \cdot Id$$

$$R = 100 \tag{28}$$

The results are illustrated in Figure 3. It can be noticed that, although a difference of 10°C was introduced in the Kalman Filter at the initial time, this one converges quickly during the

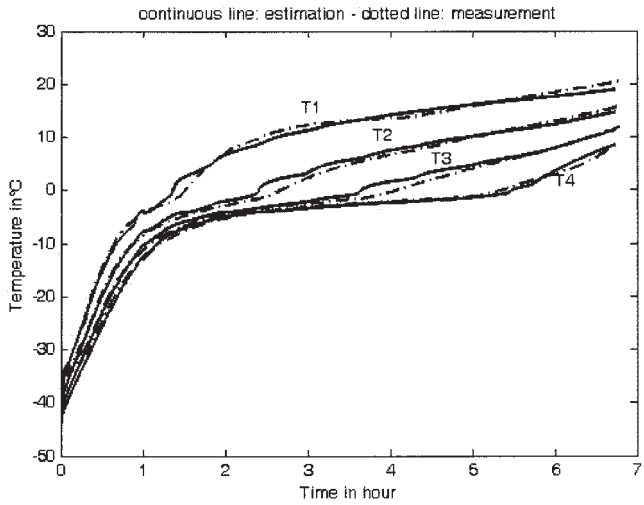

Figure 3. Experimental validation with Extended Kalman Filter

first hour. The estimation errors observed for T_2 to T_4 are relatively small. These results can be explained as follows: during the first hour of experiment, the product is totally frozen, without any melting front, as the complete state vector is observable. This period of observability is sufficiently long to allow the Kalman Filter to converge. After one hour, the melting front appears, but the weakly observable state variables are, however, correctly estimated because no disturbance occurs on the process.

Once the temperature is estimated by the Kalman filter, the location of the melting front can be deduced by interpolation or by searching the volume for which the temperature is closest to T_{m+}.

Experimental results with the switched Luenberger observers

Due to the number of volumes (equal to 7), the number of observers is 6. Indeed, contrary to the Kalman Filter, the temperature is not estimated until the melting front appears. The observers are thus designed for melting front locations corresponding to volumes 2 to 7.

For each observer, the eigenvalues were fixed to obtain a rapid convergence, leading to the values of K^{obs} mentioned in Table 2.

The results are illustrated in Figure 4. During the first hour, the difference between estimated and real values is large because, as mentioned previously, no correction is effected.

Table 2. Evolution of the Observers Gains with Switching

Melting Node	2	3	4	5	6	7
K^{obs}	$K = \begin{bmatrix} 0.054 \\ 0.455 \end{bmatrix}$	$K = \begin{bmatrix} 0.066 \\ 0.89 \\ 4.37 \end{bmatrix}$	$K = \begin{bmatrix} 0.078 \\ 1.4 \\ 11.0 \\ 38.5 \end{bmatrix}$	$K = \begin{bmatrix} 0.09 \\ 2.0 \\ 21.4 \\ 116 \\ 321 \end{bmatrix}$	$K = \begin{bmatrix} 0.10 \\ 2.68 \\ 36.0 \\ 265 \\ 1084 \\ 2577 \end{bmatrix}$	$K = \begin{bmatrix} 0.11 \\ 34.4 \\ 55.4 \\ 515 \\ 2839 \\ 9449 \\ 20059 \end{bmatrix}$

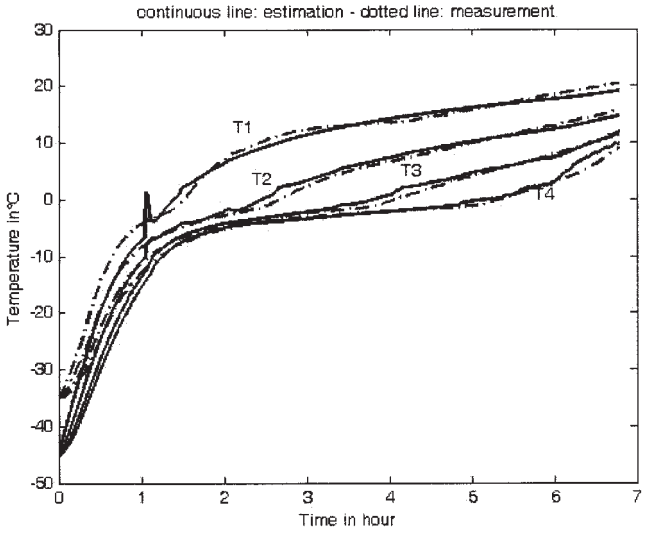

Figure 4. Experimental validation with Switched Luenberger observers

During this first hour, the temperatures are just simulated, and the initial temperature of tylose sample is -35°C while the initial temperatures in the simulator are -45°C. As soon as the measured temperature T_1 reaches the peak value ($T_{m+} = -2.6$°C), after about one hour, we can observe small disturbances in the simulated values, corresponding to the commutations.

From this point, the estimated values converge towards the measurements with a satisfying rate.

Obviously, some errors remain, but they can be attributed to uncertainties concerning the thermocouples locations, convective coefficient and of course thermal properties approximations.

Conclusion

In this article, we have proposed original approaches to estimate, in real time, the melting front progression during food thawing. The first one is based on the well-known and widely used Extended Kalman Filter. Let us however mention that, despite its great effectiveness, the Extended Kalman Filter is usually difficult to tune and requires the linearization of the system.

On the contrary, the switched reduced Luenberger observers benefits from the linearity of the observable subspace. No mathematical skills are necessary. The implementation is easy and the tuning of the gains can be performed quite quickly. A good method to determine these gains consists in calculating the eigenvalues of the matrix A^{obs} and to choose the eigenvalues of $A^{obs} - K^{obs}C^{obs}$ a little larger (in absolute value), but in a similar order of magnitude. These operations are easy to perform with Matlab®, using the commands "eig" to compute the eigenvalues, and "place" to determine K with fixed eigenvalues. Moreover, it is important to underline that the loss of observability can be more important for pure substances, because their apparent specific heat is closer to a Dirac function in the melting area. In such cases, the use of the switched observers is recommended.

It can be seen in this work that whatever is the chosen approach, satisfying results are obtained. The main advantage of the Kalman Filter is that it allows estimating the temperatures during the initial phase, without a melting front. On the contrary, the advantage of the switched linear observers lies in the fact that the melting front location can be directly deduced from the number of the active observer. An increasing of the spatial meshing, and consequently of the number of observers, would considerably improve the accuracy of this estimation.

A good improvement to the solution would be to couple these approaches, using the Kalman Filter during the first phase of the process, and, for the second, the switched observers.

Finally, this work presented results obtained during food thawing. It is important to mention that the problem presented is similar in food freezing and that the adaptation of these approaches is very simple.

Notation

x = state vector
u = input vector
y = output vector
A = state matrix
B = input matrix
C = output matrix
ρ = density ($kg.m^{-3}$)
Cp = apparent specific heat ($J.kg^{-1}.K^{-1}$)
h = convective heat transfer coefficient ($W.m^{-2}.K^{-1}$)
λ = thermal conductivity ($W.m^{-1}.K^{-1}$)
T = temperature (°C)
$T0$ = initial temperature of product (°C)
Ta = ambient temperature (°C)
L = thickness of sample (m)

Subscripts

d = defrosted
f = frozen

Literature Cited

1. Di Loreto M, Boillereaux L, Giuliani G, Conte G, Moog CH. Experimentation of melting kinetics control in a convective food thawing process. *IEEE Control System and Technology.* 2005;13:826-831.
2. Boillereaux L, Chourot JM, Havet M. Nonlinear trajectory control of high pressure thawing. *J of Process Control.* 1999;9:351-356.
3. Mannapperuma JD, Singh RP. Thawing of frozen foods in humid air. *Revue Internationale du Froid.* 1988;11:173-186.
4. Merts I, Cotter SD. A comparison of air, water and plate thawing methods for meat. In: Proceedings of the 20th International Congress of Refrigeration, Sydney, Australia. 1999;4:379.
5. Luenberger DG. An introduction to observers, *IEEE Trans on Automatic Control.* 1971;16:596-602.
6. Kalman RE, Bucy RS. New results in linear filtering and prediction theory, *Trans ASME.* 1961; 83(D):95-108.
7. Robertson DG, Lee JH. A least square formulation for state estimation, *J of Process Control.* 1995;5:291-299.
8. Rao CV, Rawlings JB, Lee JH. Constrained linear state estimation-a moving horizon approach, *Automatica,* 2001;37:1619-1628.
9. Jazwinski AH. *Stochastic Processes and Filtering Theory.* Academic Press, 1970.
10. Bornard G, Celle-Couenne F, Gilles G. Observabilité et observateurs. In: Fossard AJ, Normand-Cyrot D. Paris: Masson, Inc., 1993:177-221.
11. Gauthier JP, Hammouri H, Othman S. A simple observer for nonlinear systems. Applications to bioreactors. *IEEE Trans on Automatic Control.* 1992; 37:875-880.
12. Krener A, Isidori A. Linearization by output injection and non-linear observers. *Systems & Control Letters.* 1983;3:47-52.
13. Moreno J, Vargas A. Approximate high-gain observers for uniformly observable nonlinear systems, In: Proceedings of Conference of Decision and Control, Sydney, Australia, 2000:784-789.

14. Muske KR, Rawlings JB. Nonlinear moving horizon state estimation. In: Breber R. Ed., *Methods of Model Based Process Control*, NATO Advanced Study Institute Series: E Applied Sciences, Kluwer Academic Publishers, 1995;293:349-365.
15. Michalska H, Mayne DQ. Moving horizon observers and observers based control, *IEEE Transactions on Automatic Control.* 1995;40 :395-404.
16. Valdès-Gonzalez HM. *Contribution à l'estimation d'état à Horizon Glissant par Méthodes Ensemblistes: Applications à la Surveillance et à la Détection des Dysfonctionnements sur des Bioprocédés,* PhD Thesis, Laboratoire d'Automatique de Grenoble, Université Joseph Fourier, 2002.
17. Christofides PD. Robust control of parabolic PDE systems. *Chem Eng Sci,* 1998;53:2949-2965.
18. Xu CZ, Ligarius P, Gauthier JP. Observers for infinite dimensional dissipative bilinear systems. *Comput and Mathematics with Applications.* 1995;29:13-21.
19. Sontag E. *Mathematical Control Theory.* Springer Verlag, 1990.
20. Marino R, Tomei P, *Nonlinear Control Design.* Prentice Hall, 1995.
21. Byers R. Solving the algebraic Riccati equation with the matrix sign. *Linear Algebra and its Applications.* 1987;85:267-279.
22. Akkari E, Chevallier S, Boillereaux L. A 2D nonlinear grey-box model dedicated to microwave thawing: theoretical and experimental investigation. *Comput and Chem Eng,* in press.

Manuscript received Sept. 12, 2005, and revision received Nov. 22, 2005.